# NOTES AND CORRESPONDENCE

## Quasi-Stationary Regimes in the Northern Hemisphere of the NCAR Community Climate Model

TIMOTHY W. BARKER AND JOHN D. HOREL

*Department of Meteorology, University of Utah, Salt Lake City, Utah*

24 March 1987 and 10 September 1987

ABSTRACT

The persistence of the planetary-scale circulation in a perpetual January experiment of the NCAR Community Climate Model is investigated. Pattern correlations between maps of 500 mb geopotential height are used to identify periods in which the large scale flow remains quasi-stationary for periods of a week or longer. Thirty-one distinct periods are dominated by quasi-stationary flow patterns encompassing 22% of the model experiment. The time between quasi-stationary periods is typically longer than their duration. On the basis of subjective similarities among some of these events, we classified many of them into four distinct types. The characteristics of the model quasi-stationary regimes are contrasted with those observed and those found in simpler models.

### 1. Introduction

For decades observers have noted that the atmospheric circulation is more persistent during certain periods than during others. Most observational studies of these persistent periods have dealt with large amplitude blocking episodes that develop in preferred geographical regions. Recent observational studies of blocking episodes by Hartmann and Ghan (1980), Dole and Gordon (1983), Knox and Hay (1984), and Dole (1986) combined with numerical investigations by Lau (1983), Chen and Shukla (1983), Mullen (1985, 1986, 1987) and Blackmon et al. (1986) have shed considerable light on the regional balances and flow characteristics during these events. Numerical studies of wave–mean flow and wave–wave interactions have shown that in the presence of constant external forcing, model atmospheres can equilibrate into numerous different flow patterns (for a review of this work, see Legras and Ghil, 1985; Reinhold, 1987; Ghil and Childress, 1987). Some of these stable patterns resemble blocking episodes while others consist of increased zonal flow or low amplitude anomalous flow patterns.

An earlier study by Horel (1985, hereafter referred to as H) identified quasi-stationary events in the observed planetary circulation of the Northern Hemisphere during 17 winter seasons. In that study, the identification of hemispheric stationary patterns was based upon pattern correlations between maps of the observed height of the 500 mb pressure surface. This approach identified both large and small amplitude flow patterns which remained stationary over major portions of the Northern Hemisphere, not just large amplitude regional flow patterns such as blocking.

In this paper, we investigate the persistence and identify quasi-stationary events in a 1200-day record from a perpetual January experiment of the National Center for Atmospheric Research (NCAR) Community Climate Model (CCM), version 0-A. The reason for this investigation is threefold. First, combined with the results of H, this analysis provides a measure of the ability of the CCM to simulate the observed atmosphere adequately. Second, the quasi-stationary events identified in a complex general circulation model such as the CCM can be compared to similar events in simpler models. Finally, the perpetual January experiment provides a controlled environment with fixed lower boundary conditions which aids in the interpretation of the dynamical processes responsible for quasi-stationary events.

### 2. Data processing

The CCM is a sigma coordinate, spectral model with rhomboidal truncation at wavenumber 15. There are nine model levels at 40 Gaussian latitudes and 48 longitudinal grid points giving approximately a 4.4° × 7.5° latitude/longitude grid. Further details about the CCM can be found in McAveny et al. (1978) and Ramanthan et al. (1983). The performance of the model in the CCM0-A perpetual January experiment has been studied by Pitcher et al. (1983) and Malone et al. (1984). They found that, for the most part, the model simulates the large-scale time-mean features and variability of the atmosphere quite well.

The model experiment extends over a 1400-day period, of which the last 1200 days are analyzed here.

*Corresponding author address:* Dr. John D. Horel, Department of Meteorology, The University of Utah, 819 Wm. C. Browning Bldg., Salt Lake City, UT 84112.

The analysis procedure follows closely the procedure of H. Twice daily 500 mb height maps were averaged together to obtain daily 500 mb height maps for the 1200 day period. These daily maps will be referred to as being "unfiltered". Wavenumbers greater than 4 were eliminated along each latitude circle to emphasize planetary scale waves and reduce the effect of synoptic scale transient waves. The time series of geopotential height exhibited no significant linear trends over the lifetime of the model experiment. For direct comparison with the observational results, the data were interpolated to the Northern Hemisphere polar stereographic grid of the National Meteorological Center. Standardized anomalies were then calculated at each grid point by subtracting the 1200-day mean from each daily value and dividing by the standard deviation at that grid point. This standardization procedure insures that anomalies are given equal weight over all geographic regions rather than the greatest weight being given to anomalies in the storm track regions. Hereafter, the height anomalies resulting from the above analysis procedure will be referred to as "standardized" height anomalies.

If the standardized height anomaly at a gridpoint $x$ and time $t$ is indicated by $Y(x, t)$, then the pattern correlation $p(t, \tau)$ between the maps on day $t$ and day $t - \tau$ is defined here as follows:

$$p(t, \tau) = \langle Y(x, t)Y(x, t - \tau)\rangle / s_p(t)s_p(t - \tau)$$

where $s_p^2(t) = \langle Y(x, t)Y(x, t)\rangle$ and $\langle \ldots \rangle$ indicates a spatial average over the area from 20°N to the North Pole which is weighted such that each grid point represents an equal area on a sphere. As described by H, the above definition of the pattern correlation differs from its usual definition since $Y(x, t)$ and $Y(x, t - \tau)$ are not departures from the spatial averages $\langle Y(x, t)\rangle$ and $\langle Y(x, t - \tau)\rangle$. This definition of pattern correlation does not significantly influence the results of this study since the hemispheric spatial averages, $\langle Y(x, t)\rangle$, are close to zero.

## 3. Results

Time series of pattern correlations between maps separated by $\tau$ days were created for $\tau$ equal to 1, 2, 3, 5, 7, 10, 12 and 15 days. As expected, these time series show that the correlations between pairs of maps separated by only 1 or 2 days are very high and positive whereas correlations between pairs of maps separated by 5 or more days are much smaller and occasionally negative. Due to space limitations, we only show in Fig. 1 the time series for a lag of 5 days. This time series exhibits many of the same features observed in the real atmosphere by H. It shows numerous periods when the correlation between maps 5 days apart is above 0.5 as well as many periods when the correlation is much less. The average 5-day lag correlation is 0.33, which is nearly equal to the average of the observed 5-day lag correlation (0.34). Generally, at all lags the mean correlations are slightly less in the model data than those observed. Frequency distributions of the correlations about these means show further that the model atmosphere is slightly less persistent than the observed atmosphere (not shown). Less persistence in the 500 mb height field of the CCM model than in the observed atmosphere was also observed in an experiment using a version of the CCM developed by Chervin (1986) which incorporates an annual cycle in external variables (van den Dool and Chervin, 1986).

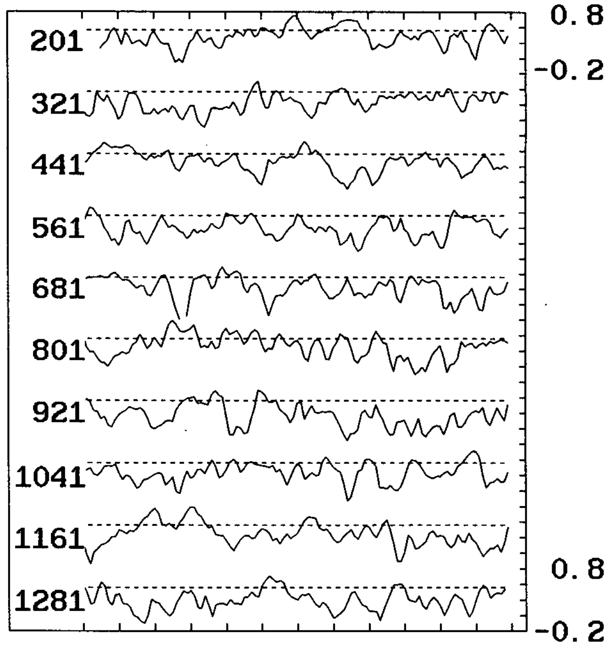


FIG. 1. Correlations between pairs of anomaly maps separated by 5 days. Only correlations during the last 1200 model days are shown. The numbers in the left margin indicate the first day plotted on each line. Tick marks on the top and bottom of the figure denote intervals of 10 days. The dashed line indicates correlation of 0.5. Values less than −0.2 are not plotted.

Figure 1 indicates many periods exist when the model planetary circulation undergoes a rapid readjustment from one flow pattern to another. In Fig. 2 we show the daily standardized anomaly maps during one such period. On model day 957 (Fig. 2a) the major features dominating the Northern Hemisphere are large positive height anomalies over the North Atlantic and Middle East and large negative height anomalies over the subtropical Atlantic and Europe. These features, along with most of the other hemispheric features, changed only slightly during the next few days (Fig. 2b, c). However, five days later the model atmosphere appears much different: on model day 962 (Fig. 2d), the positive height anomalies over the North Atlantic weakened and the negative height anomalies over Europe progressed eastward about 20°. In addition, a wavetrain of alternating centers of positive and negative height anomalies extends around much of the Northern

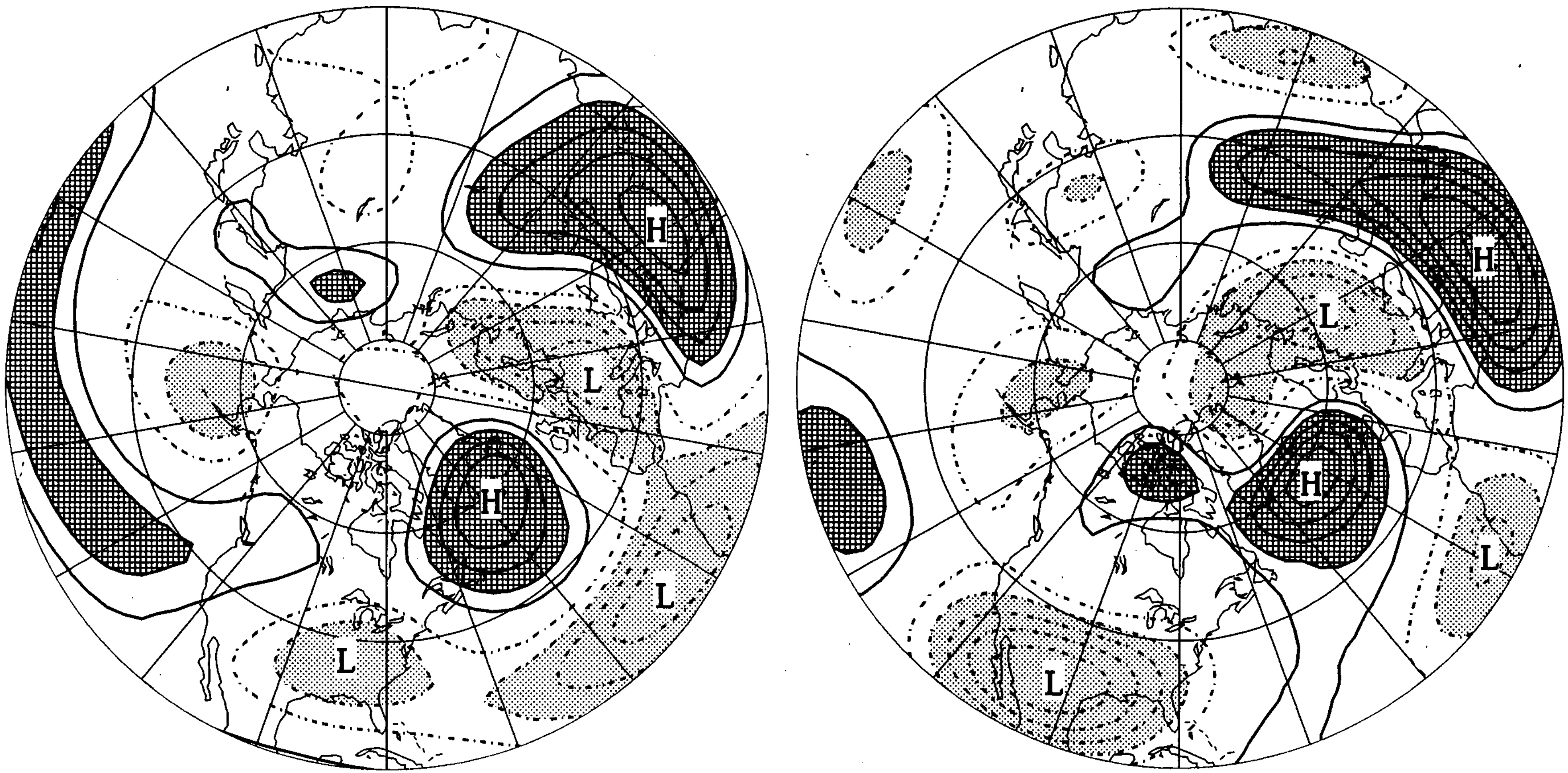


FIG. 2. Daily filtered, standardized anomaly maps of 500 mb geopotential height: (a) day 957; (b) day 959; (c) day 960; and (d) day 962. The contour interval is 0.5 with positive contours solid (negative contours dashed), and the zero contour omitted. Values above +1.0 (below −1.0) are crosshatched (stippled).

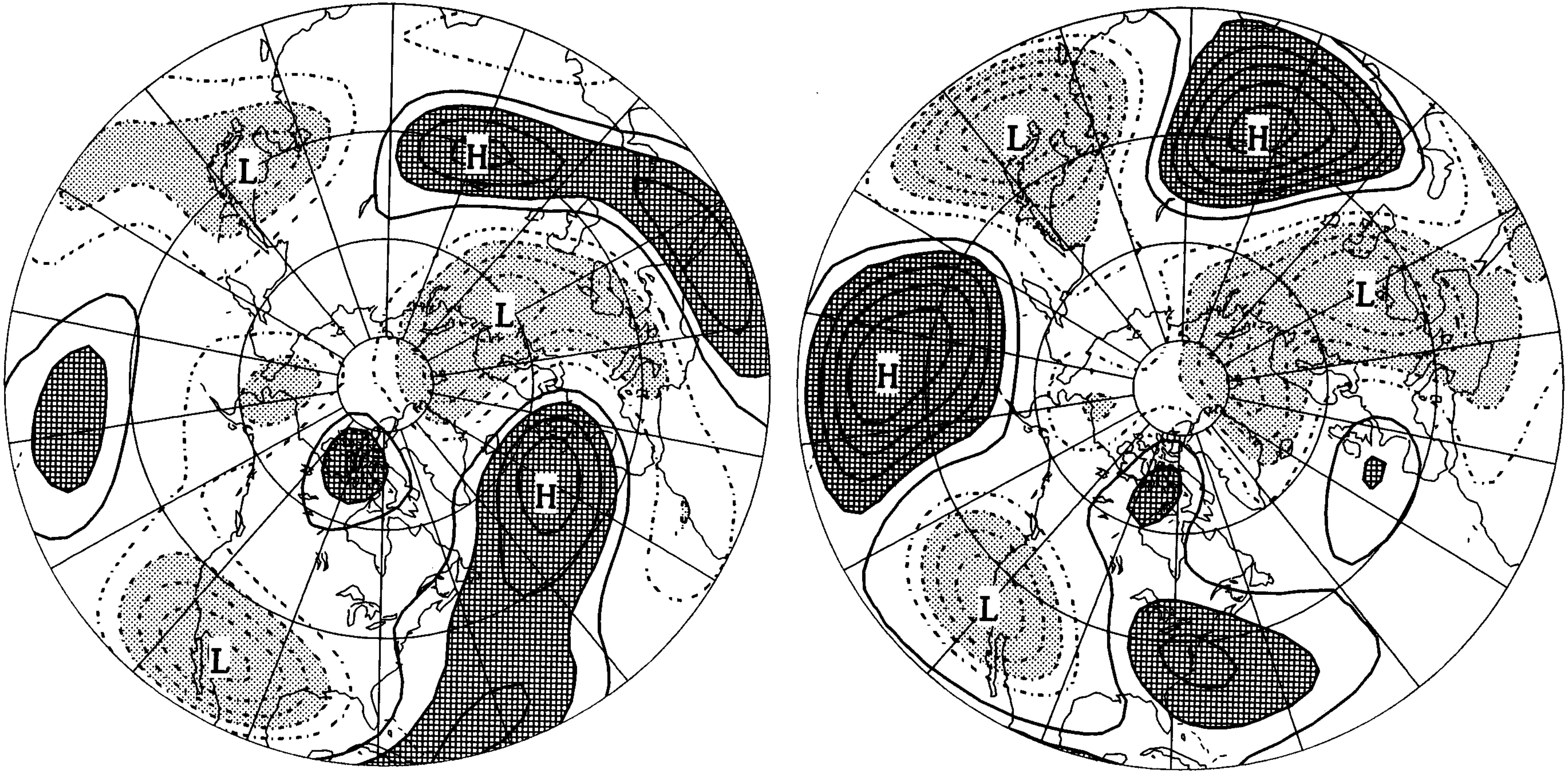


FIG. 2. (*Continued*)

Hemisphere. As evident in Fig. 1, the 5-day lag pattern correlation between the maps on day 962 and 957 is only −0.05, indicative of the rapid change in the planetary circulation.

By itself, high correlation between maps several days apart does not imply that the atmosphere is persistent, since some transient flow pattern may exist during the intervening days. To identify periods that are truly persistent, we again follow the procedure of H. We consider a series of maps to be quasi-stationary if the pattern correlations between all maps in a 7-day (or longer) series remain above 0.5. Although this definition is quite arbitrary, our experience suggests that maps which are correlated with each other in excess of 0.5 have nearly all their major features in common. Furthermore, the pattern correlations were transformed using the Fisher-*z* transformation so that they resemble more closely a normally distributed population. Following the procedure of H, the pattern correlations at all lags indicate that there are between 21 and 31 spatial degrees of freedom over the Northern Hemisphere. Even with a conservative estimate of 20 independent gridpoints, a correlation of 0.5 is significant at the 5% level. One drawback of the above approach is that it identifies many overlapping stationary events; in these cases we subjectively chose the ones with the longest duration. The dates and durations of the 31 events we identified are shown in Table 1.

The events encompass 268 (22%) of the 1200 model days which is slightly less than the 25% of observed days found to be within quasi-stationary events during 17 winters. The average duration of the model quasi-stationary events is 8 days. With the continuous model data, we are able to investigate the duration of transient periods between quasi-stationary events (see Table 1) which cannot be properly investigated in the observed data. Naturally, since the events account for only 22% of the model days, the time between events is, on average, substantially longer than the residence times in quasi-stationary patterns. Further, because of the large differences in the length of these periods, it appears that there is no preferred duration of transitory periods.

We averaged separately, over the duration of each event listed in Table 1, the unfiltered 500 mb height maps and standardized anomaly maps used in the above analysis. The resulting composite maps provide an indication of the prevailing flow during each quasi-stationary event. Like the events identified in the observed wintertime circulation, the model's quasi-stationary events have considerable spatial diversity. In Fig. 3a we show the composite of the standardized anomaly maps for the period from day 952 through day 960. This composite has several dominant features primarily in the Atlantic–Europe sector: positive height anomalies over the North Atlantic and the Middle East, and negative height anomalies over the southern United States, subtropical Atlantic, and Europe. All of these features are evident in the individual daily maps on days 957, 959 and 960 shown in Fig. 2, although the relative amplitudes of the various features differ during the period. In Fig. 3b we show the composite of the unfiltered 500 mb height maps during this same period. Deep troughs upstream and downstream of the strong ridge over the North Atlantic are particularly evident and correspond well with the anomaly pattern shown in Fig. 3a. This correspondence between Figs. 3a and 3b which are generated from filtered and unfiltered data respectively, also indicates that our filtering of the standardized anomalies has not significantly altered the character of the flow pattern during the event.

Composites of the event which began only four days after that shown in Figs. 3a, b are presented in Figs. 3c, d. Many of its features are the opposite of those in the previous event: negative height anomalies over the North Atlantic and Caribbean, and positive height anomalies over the subtropical Atlantic, eastern Europe and eastern Canada (Fig. 3c). Despite the fact that only four days separate these two events, the correlation between their composite anomaly maps is −0.38. The differences in the actual flow patterns between these

TABLE 1. Starting day and duration of quasi-stationary events identified in the last 1200 days of the perpetual January experiment of the NCAR CCM as well as the number of days between neighboring events. Classification of events as Pacific–North American Negative (PNA−), wavenumber 1 (WV1), wavenumber 2 (WV2), Atlantic Positive (A+), and Atlantic Negative (A−) is also indicated.

| Starting day | Duration | Intervening days | Classification |
|---|---|---|---|
| 242 | 7 | 4 | PNA− |
| 253 | 11 | 4 | PNA− |
| 268 | 10 | 32 | PNA− |
| 310 | 7 | 46 | |
| 363 | 8 | 17 | |
| 388 | 8 | 22 | WV1 |
| 418 | 7 | 15 | |
| 440 | 11 | 8 | A+ |
| 459 | 7 | 31 | A+ |
| 497 | 9 | 52 | |
| 558 | 9 | 29 | PNA− |
| 596 | 8 | 56 | |
| 660 | 7 | 17 | WV1 |
| 684 | 8 | 6 | |
| 698 | 7 | 10 | |
| 715 | 10 | 97 | PNA− |
| 822 | 12 | 1 | WV2 |
| 835 | 11 | 22 | WV2 |
| 868 | 8 | 2 | PNA− |
| 878 | 7 | 67 | |
| 952 | 9 | 4 | A+ |
| 965 | 9 | 130 | A− |
| 1104 | 7 | 4 | WV1 |
| 1115 | 8 | 5 | WV1 |
| 1128 | 8 | 7 | WV1 |
| 1143 | 10 | 30 | WV1 |
| 1183 | 11 | 25 | WV2 |
| 1219 | 9 | 12 | WV2 |
| 1240 | 7 | 82 | PNA− |
| 1329 | 10 | 24 | |
| 1363 | 8 | — | |

events is quite striking (Figs. 3b, d): split flow over eastern North America and Europe replace the deep troughs evident earlier. During the short transition between these two events, the height and anomaly maps differ markedly from those of either event (Fig. 2d).

On the basis of similarities among some of the events, we subjectively classified many of them into four distinct "regimes" as summarized in Table 1. We averaged the composite maps for all similar events to give a general idea of the structure of each event. These regime composites, shown in Fig. 4, have much less amplitude than the individual composites because the individual events differ slightly in the amplitude and position of their dominant features. Admittedly, this classification is subjective but it is intended to show some of the similarities among the 31 events in a compressed format.

Seven of the individual quasi-stationary events have anomaly patterns which, in the Pacific sector, resemble the negative phase of the Pacific–North American (PNA) teleconnection pattern identified in the observed atmosphere by Wallace and Gutzler (1981): positive height anomalies in the Aleutian region, and negative height anomalies near Hawaii and over western North America (Fig. 4a). A Student's t test was applied to the ensemble average as shown in Fig. 4a; all of the dominant features of the composite pass the Student's t test at the 5% level. An additional six events have a wavenumber 1 pattern at high latitudes (labeled WV1) as evidenced by positive height anomalies over Europe and negative height anomalies near the International Dateline at a latitude of about 60°N. These events also have positive height anomalies over much of the subtropical eastern hemisphere which lead to somewhat enhanced zonal flow in the middle latitudes (Fig. 4b). As in Fig. 4a, the dominant features of the composite pass the Student's t test at the 5% level.

Four other events are dominated by a wavenumber 2 pattern (labeled WV2) with positive height anomalies over eastern Asia and the North Atlantic, and negative height anomalies to the south of these areas (Fig. 4c). In addition, three events are similar in the Atlantic sector (labeled A+) with negative height anomalies over North America and Europe, and positive height anomalies over the North Atlantic and the Middle East (Fig. 4d). The event shown in Figs. 3a, b falls into this category while that in Figs. 3c, d is roughly the inverse (labeled A−). While the dominant features in the composites of Figs. 4c and 4d pass the Student's t test, we felt that because of the limited samples involved, shading those areas would be misleading. The remaining events did not resemble each other closely enough to justify classification and hence all of these are left uncategorized.

Quasi-stationary events of the same type often follow one another separated by short transient periods (see Table 1). For example, the first three events identified in the model experiment are all of the PNA-type and they are separated by only four days each. Starting on day 1104, the WV1 type of event occurs four times separated by transient periods lasting 4, 5, and 7 days. Examination of the anomaly and 500 mb height maps during the transient periods between recurring types of events reveal that these intervening periods are indeed the result of significant fluctuations in the hemispheric circulation and not simply a result of the criteria used to define the quasi-stationary events.

## 4. Discussion

The results of the previous section are encouraging for several reasons. The lag correlation statistics indicate that the perpetual January experiment of the CCM reasonably reproduces many aspects of the temporal variability of the wintertime circulation in the Northern Hemisphere. Our analysis of daily model output is able to provide some additional information that is often obscured by conventional approaches employing 5-day, monthly or seasonal averages; the pattern correlations between daily maps provide a measure of model persistence without regard to geographic location or amplitude of the flow pattern.

Mullen (personal communication, 1987) identified blocking episodes in this same model experiment using the criteria applied in his earlier studies (Mullen 1985, 1986, 1987) with the exception that only zonal wavenumbers 1–4 were retained; processed in this manner his results can be contrasted to ours. He found a total of 21 blocking events in the Pacific sector and eight events in the Atlantic sector. Of these 29 blocking events, eight of them overlap with quasi-stationary periods identified here. Thus, regional blocking episodes are often accompanied by more variable flow in other parts of the hemisphere. In addition, blocking episodes are not the only type of quasi-stationary flow pattern observed in this model experiment. Although the frequency of occurrence and lifetime of quasi-stationary events are somewhat sensitive to our criteria used to define them, we believe that our results are a conservative estimate of the patterns that synopticians would regard subjectively as being stationary for periods of a week or longer.

The identification of similarities among some of the quasi-stationary events in the NCAR CCM corroborates earlier numerical work using simpler models (Charney and Devore, 1979; Legras and Ghil, 1985; Mo and Ghil, 1986). In those barotropic model experiments investigating mean flow–wave and wave–wave interactions, the model atmospheres equilibrate into a few preferred flow regimes, similar in many respects to those identified here. In this experiment, using a global primitive equation model with fixed external boundary conditions, nonlinear interactions in the planetary-scale circulation undoubtedly play an important role in generating quasi-stationary events. Put another way, our results indicate that even without

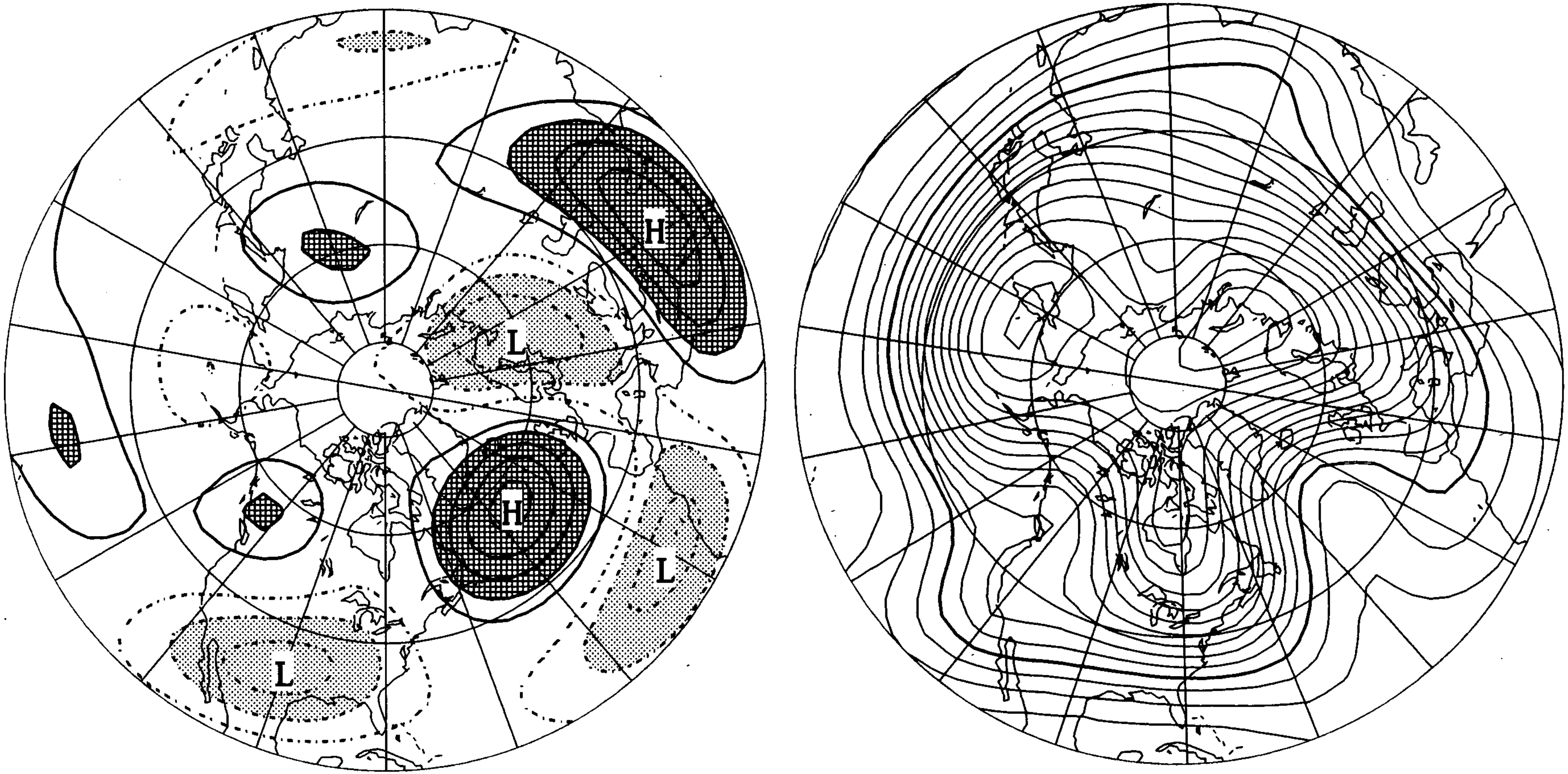


FIG. 3. (a) Composite of the filtered, standardized anomaly maps for the regime beginning on day 952. The contour interval is 0.5 with positive contours solid (negative contours dashed) and the zero contour omitted. Values above +1.0 (below −1.0) are crosshatched (stippled). (b) Composite of the unfiltered 500 mb height for the regime beginning on day 952. The contour interval is 60 m and the 5580 m contour is high-lighted. (c) As in (a) except for the regime beginning on day 965. (d) As in (b) except for the regime beginning on day 965.

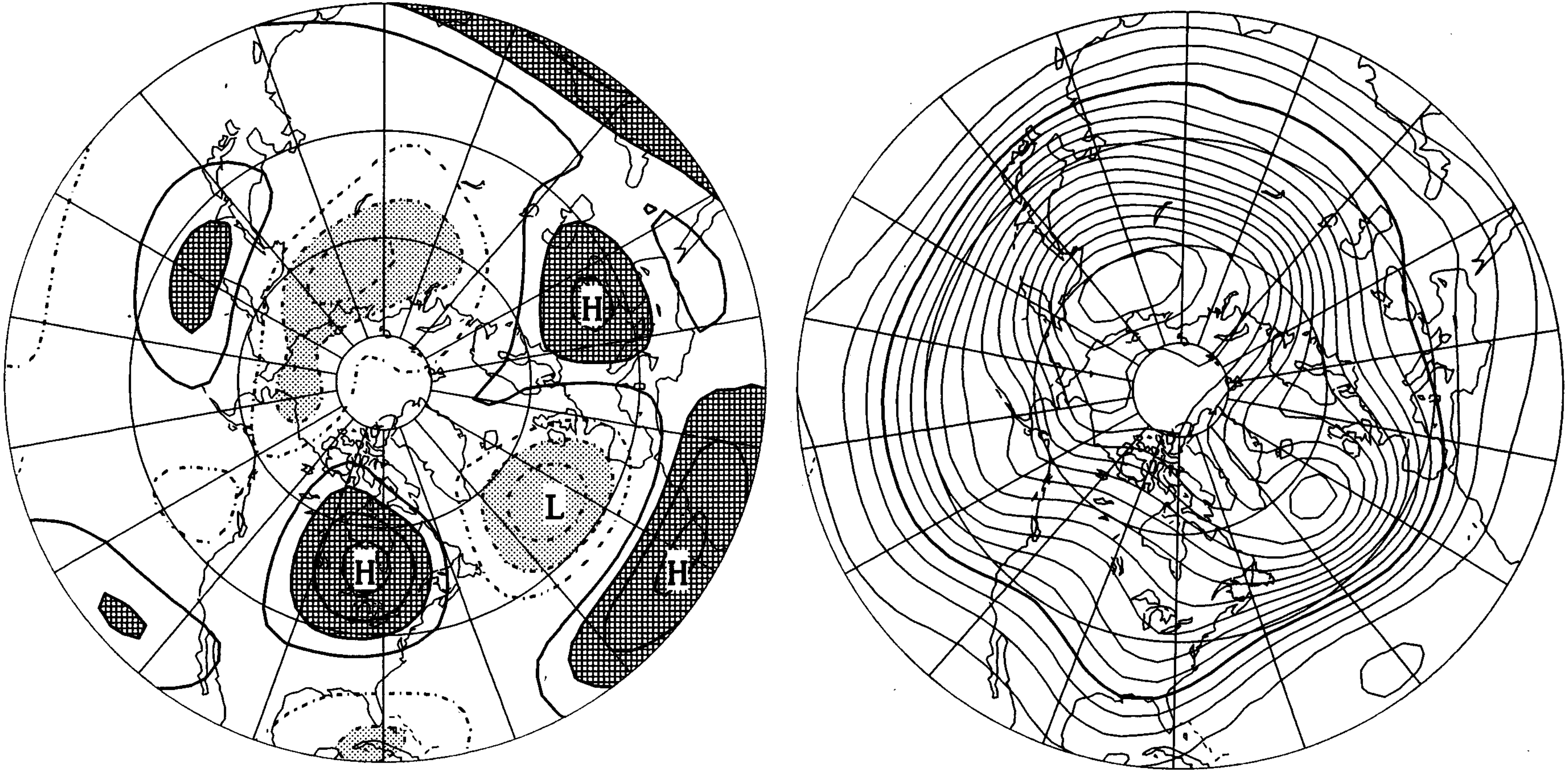


FIG. 3. (*Continued*)

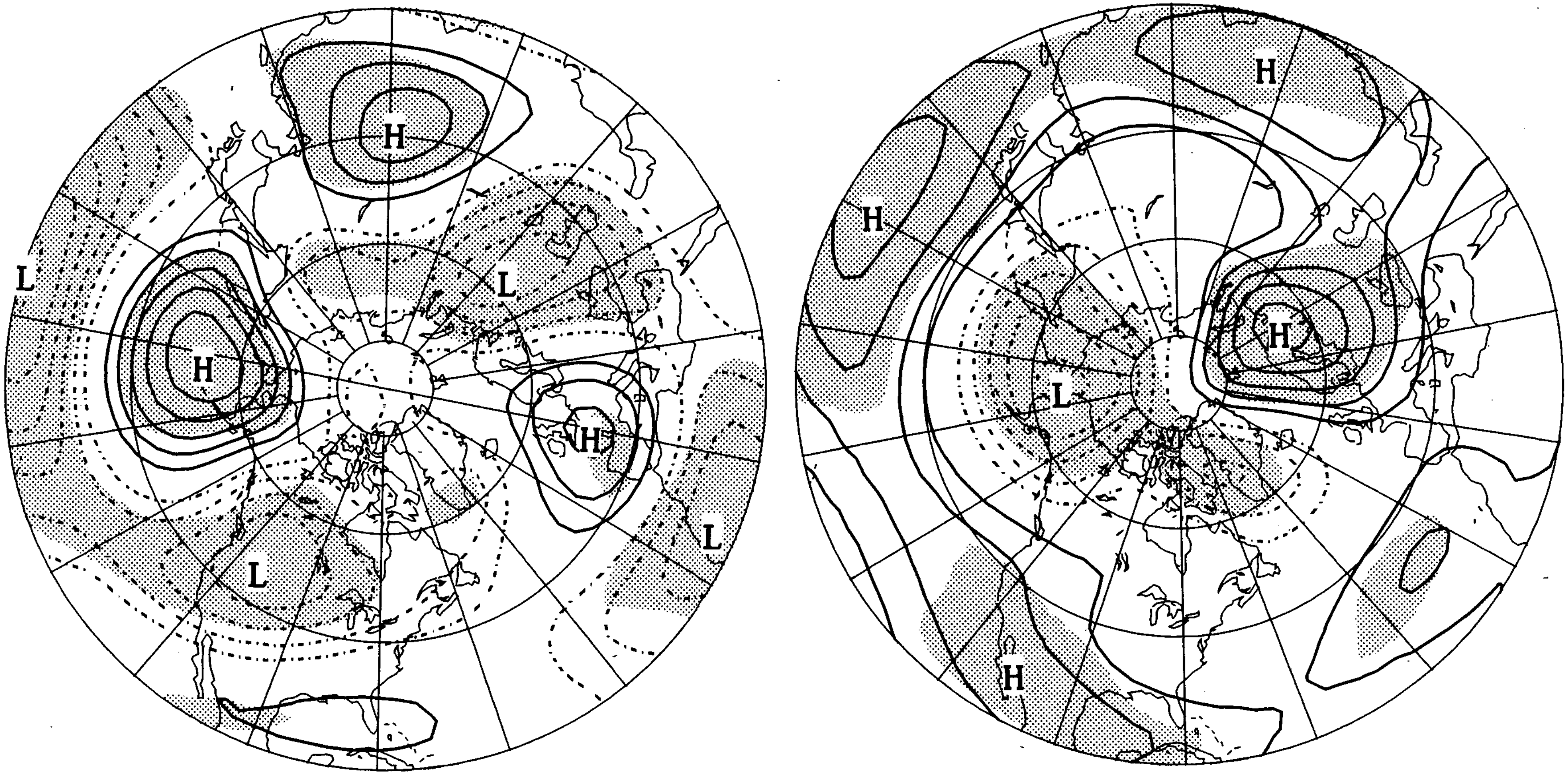


FIG. 4. Ensemble average of regime composites for similar types of regimes: (a) Pacific–North America Negative regimes (PNA−); (b) wavenumber 1 regimes (WV1); (c) wavenumber 2 regimes (WV2); and (d) Atlantic Positive regimes (A+). The contour interval is 0.25 with positive contours solid (negative contours dashed) and the zero contour omitted. Areas where the ensemble averages pass the Student's t test at the 5% level are stippled in (a) and (b) (see text).

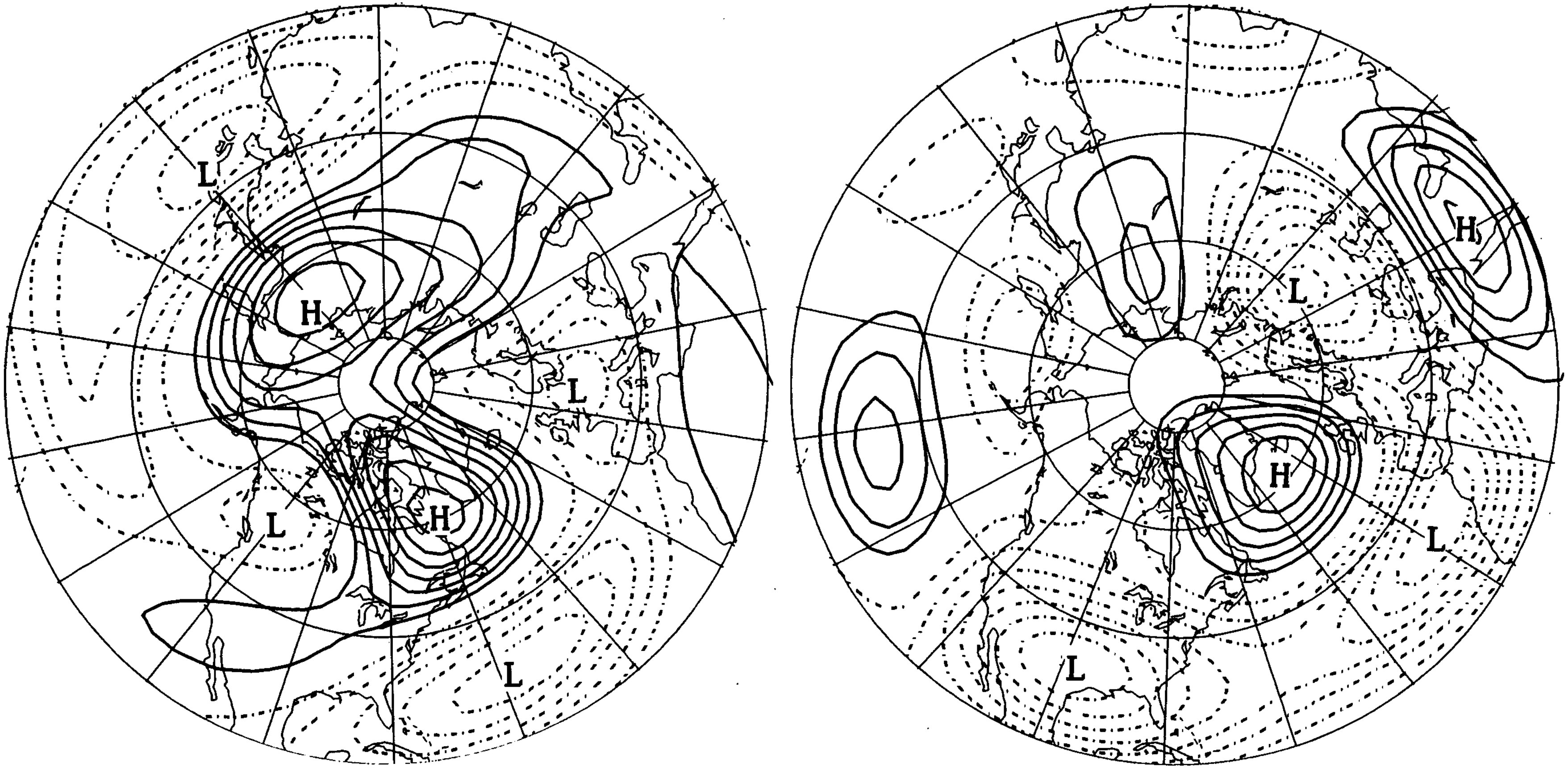


FIG. 4. (*Continued*)

anomalous boundary forcing, the model atmosphere is capable of developing considerable medium frequency variability.

The barotropic model results leave one with the impression that the atmosphere resides nearly continuously in quasi-stationary flow patterns, i.e., the time between such events is relatively short in comparison to their duration. As the model complexity increases (Reinhold and Pierrehumbert, 1982; Roads, 1985), the number of quasi-stationary events decreases and the time between such events lengthens. Our results indicate that occasionally the NCAR CCM undergoes rapid transitions from one type of event to another and similar results were found in the observed circulation (H). However, as a general rule, both observed and simulated quasi-stationary events tend to be of shorter duration than the intervening transient periods.

An intriguing result of our analysis is the occasional periods during which similar events recur several times in a row separated by short transient periods (see Table 1). If a monthly average was computed for the period from day 240 to 270 (day 1100 to 1130), then the resulting flow would resemble strongly the PNA− (WV1) pattern. On the other hand, a monthly average encompassing the period from day 950 to 980 would exhibit a weak signal since the flow nearly reversed itself within this period (see Fig. 3). Hence, the low frequency variability in the model can be partially explained in terms of the constructive and destructive superposition of quasi-stationary events. As noted by Chervin (1986), the amplitude of this low-frequency variability can be quite large even when the model's external forcing is fixed.

Although the numerous events identified here show a great deal of spatial diversity, among those events which have some similarities, patterns resembling the negative phase of the Pacific–North American teleconnection pattern (weaker than normal zonal flow across the North Pacific) occur most often. The phase of the PNA pattern on monthly averaged time scales has been associated with variations in midlatitude and tropical sea surface temperature variations (Namias, 1978; Horel and Wallace, 1981). One interpretation of our results is that the negative phase of the PNA pattern is sensitive to variations in diabatic heating over the maritime continent region (Simmons et al., 1983), a climatologically active area for convection which is well simulated in this perpetual January experiment (Branstator, 1985).

As suggested by many of the studies on nonlinear interactions (Charney and Devore, 1979; Legras and Ghil, 1985), low-frequency changes in the external boundary conditions may predispose the planetary circulation towards particular quasi-stationary patterns. The recurrence of the negative phase of the PNA pattern and total absence of the positive phase of the PNA pattern as a quasi-stationary pattern in this "control" experiment with fixed climatological mean sea surface temperatures help to explain the large statistically significant response found in similar perpetual January experiments of the NCAR CCM in which SST anomalies are added in the tropical Pacific (Blackmon et al., 1983; Geisler et al., 1985; Blackmon et al., 1987).

*Acknowledgments.* This research was supported by the Climate Dynamics Program of the National Science Foundation under Grant ATM 85-05426. We would like to thank L. Buja, University of Utah, and E. Pitcher, University of Miami, for their help in obtaining the data, and S. Mullen, University of Michigan, J. Geisler, University of Utah, H. van den Dool, Climate Analysis Center, and the reviewers for their comments on earlier versions of this paper.

REFERENCES

Blackmon, M. L., J. E. Geisler and E. J. Pitcher, 1983: A general circulation study of January climate anomaly patterns associated with interannual variation of equatorial Pacific sea surface temperatures. *J. Atmos. Sci.*, **40**, 1410–1425.

——, S. L. Mullen and G. T. Bates, 1986: The climatology of blocking events in a perpetual January simulation of a spectral general circulation model. *J. Atmos. Sci.*, **43**, 1379–1405.

——, G. W. Branstator, G. T. Bates and J. E. Geisler, 1987: An analysis of equatorial Pacific sea surface temperature anomaly experiments in general circulation models with and without mountains. *J. Atmos. Sci.*, **44**, 1828–1844.

Branstator, G., 1985: Analysis of general circulation model sea-surface temperature anomaly simulations using a linear model. Part II: Eigenanalysis. *J. Atmos. Sci.*, **42**, 2242–2254.

Charney, J. G., and J. G. Devore, 1979: Multiple flow equilibria in the atmosphere and blocking. *J. Atmos. Sci.*, **36**, 1205–1216.

Chen, T.-C., and J. Shukla, 1983: Diagnostic analysis and spectral energetics of a blocking event in the GLAS climate model simulation. *Mon. Wea. Rev.*, **111**, 3–22.

Chervin, R. M., 1986: Interannual variability and seasonal climate predictability. *J. Atmos. Sci.*, **43**, 233–251.

Dole, R. M., 1986: Persistent anomalies of the extratropical Northern Hemisphere wintertime circulation: structure. *Mon. Wea. Rev.*, **114**, 178–207.

——, and N. D. Gordon, 1983: Persistent anomalies of the extratropical Northern Hemisphere wintertime circulation: Geographical distribution and regional persistence characteristics. *Mon. Wea. Rev.*, **111**, 1567–1586.

Geisler, J. E., M. L. Blackmon, G. T. Bates and S. Muñoz, 1985: Sensitivity of January climate response to the magnitude and position of equatorial Pacific sea surface temperature anomalies. *J. Atmos. Sci.*, **42**, 1037–1049.

Ghil, M., and S. Childress, 1987: *Topics in Geophysical Fluid Dynamics: Atmospheric Dynamics, Dynamo Theory, and Climate Dynamics.* Springer-Verlag, 485 pp.

Hartmann, D. L., and S. J. Ghan, 1980: A statistical study of the dynamics of blocking. *Mon. Wea. Rev.*, **108**, 1144–1159.

Horel, J. D., 1985: The persistence of the 500 mb height field during Northern Hemisphere winter. *Mon. Wea. Rev.*, **113**, 2030–2042.

——, and J. M. Wallace, 1981: Planetary-scale atmospheric phenomena associated with the Southern Oscillation. *Mon. Wea. Rev.*, **109**, 813–829.

Knox, J. L., and J. E. Hay, 1984: Blocking signatures in the Northern Hemisphere: Rationale and identification. *Atmosphere; Atmos.-Ocean,* **22**, 36–47.

Lau, N.-C., 1983: Mid-latitude wintertime circulation anomalies appearing in a 15-year GCM experiment. *Large-Scale Dynamical Processes in the Atmosphere,* B. J. Hoskins and R. P. Pearce, Eds., Academic Press, 397 pp.

Legras, B., and M. Ghil, 1985: Persistent anomalies, blocking and variations in atmospheric predictability. *J. Atmos. Sci.,* **42,** 433–471.

Malone, R. C., E. J. Pitcher, M. L. Blackmon, K. Puri and W. Bourke, 1984: The simulation of stationary and transient geopotential-height eddies in January and July With a spectral general circulation model. *J. Atmos. Sci.,* **42,** 1394–1419.

McAvaney, B. J., W. Bourke and K. Puri, 1978: A global spectral model for simulation of the general circulation. *J. Atmos. Sci.,* **35,** 1557–1583.

Mo, K. C., and M. Ghil, 1987: Statistics and dynamics of persistent anomalies. *J. Atmos. Sci.,* **44,** 877–901.

Mullen, S. L., 1985: On the maintenance of blocking anticyclones in a general circulation model, NCAR, Cooperative thesis No. 86. [Available from NCAR, P.O. Box 3000, Boulder CO 80307.]

——, 1986: The local balances of vorticity and heat for blocking anticyclones in a spectral general circulation model. *J. Atmos. Sci.,* **43,** 1406–1441.

——, 1987: Transient eddy forcing of blocking flows. *J. Atmos. Sci.,* **44,** 3–22.

Namias, J., 1978: Multiple causes of the North American abnormal winter 1976–77. *Mon. Wea. Rev.,* **106,** 279–295.

Pitcher, E. J., R. C. Malone, V. Ramanathan, M. L. Blackmon, K. Puri and W. Bourke, 1983: January and July simulations with a spectral general circulation model. *J. Atmos. Sci.,* **40,** 580–604.

Ramanathan, V., E. J. Pitcher, R. C. Malone and M. L. Blackmon, 1983: The response of a spectral general circulation model to refinements in radiative processes. *J. Atmos. Sci.,* **40,** 605–630.

Reinhold, B. B., 1987: Weather regimes: The challenge in extended-range forecasting. *Science,* **235,** 437–441.

——, and R. T. Pierrehumbert, 1982: Dynamics of weather regimes: Quasi-stationary waves and blocking. *Mon. Wea. Rev.,* **110,** 1105–1145.

Roads, J. O., 1985: Temporal variations in predictability. *J. Atmos. Sci.,* **37,** 1957–1967.

Simmons, A. J., J. M. Wallace and G. W. Branstator, 1983: Barotropic wave propogation and instability, and atmospheric teleconnection patterns. *J. Atmos. Sci.,* **40,** 1363–1392.

Wallace, J. M., and D. S. Gutzler, 1981: Teleconnections in the geopotential height field during the Northern Hemisphere winter. *Mon. Wea. Rev.,* **109,** 784–812.

van den Dool, H. M., and R. M. Chervin, 1986: A comparison of month-to-month persistence of anomalies in a general circulation model and in the earth's atmosphere. *J. Atmos. Sci.,* **43,** 1454–1466.